Supporting Information

Highly soluble gadofullerene salt and its magnetic property

YongqiangFeng[‡a], JieLi[‡a], Zhuxia Zhang[b], Bo Wu[a], Yongjian Li[a], Li Jiang[a], Chunru Wang[a], and Taishan Wang*[a]

[a]*Beijing National Laboratory for Molecular Sciences, Laboratory of Molecular Nanostructure and Nanotechnology, Institute of Chemistry, Chinese Academy of Sciences, Beijing 100190, China*
E-mail: wangtais@iccas.ac.cn
[b] *Key Laboratory of Interface Science and Engineering in Advanced Materials, Taiyuan University of Technology, Ministry of Education, Research Center of Advanced Materials Science and Technology, Taiyuan University of Technology, Taiyuan 030024, China*

Contents

Figure S12. Aggregated Gd@C_{82} powder in ODCB (left) and ODCB solution of Gd@C_{82} with 1 eq. of TBPA (right).

Figure S13. Optical images of solutions of Gd@C_{82} in $CHCl_3$, MeCN, EtOAc, Pyridine, and THF (from left to right in sequences).

Figure S14. UV-Vis spectra of Gd@C_{82}/TBPA before (black) and after (red) hydrolysis.

Figure S15. SEM images of the Gd@C_{82}/TBPA-PVP composite film fabricated by electrospinning with a PVP ($M_n \approx 30\ 000$) concentration of a) 5% and b) 7%.

Figure S16. X-band EPR spectra of Gd@C_{82} and TBPA mixture measured at 173 K.

Experimental Section:

1. The synthesis and purification of Gd@C_{2v}-C_{82}

The Gd@C_{2v}-C_{82} was synthesized by arc-discharging method. Briefly, the mixture of graphite powder and Gd/Ni_2 alloy with a mass ratio of 1:3 was packed into core-drilled graphite rods. Subsequently the rods were burnt in a Krätschmer-Huffman generator under an atmosphere of 450 Torr He. The as-prepared soot was Soxlet-extracted with DMF for 24 h. Gd@C_{2v}-C_{82} was isolated and purified by multi-step high performance liquid chromatography (HPLC) with toluene as eluent. Figure S1-S3 show multi-step HPLC profiles of Gd@C_{2v}-C_{82}. The purity of the isolated Gd@C_{2v}-C_{82} was confirmed by matrix-assisted laser desorption/ionization time of flight mass spectrometry (MALDI-TOF-MS), see Figure S4.

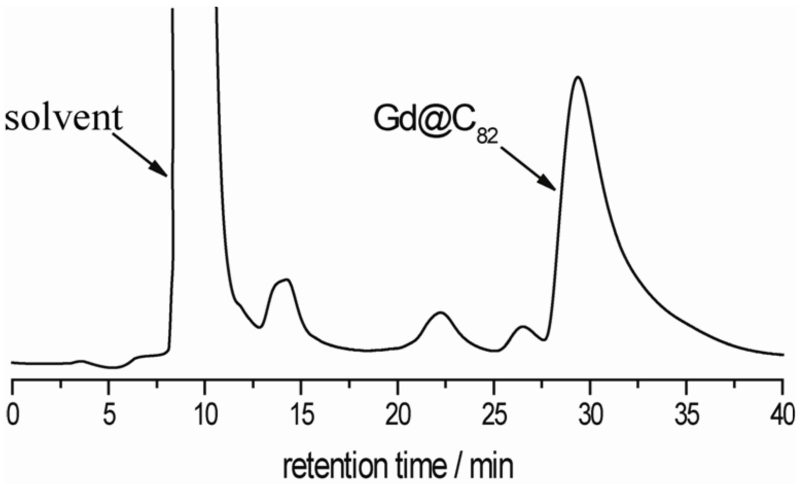

Figure S1. The first-step separation of Gd@C_{2v}-C_{82} on a Buckyprep-M column. (Chromatographic column 20 × 250 mm; toluene as eluent; 12 mL/min). The DMF extracted solution was concentrated and redissolved in toluene.

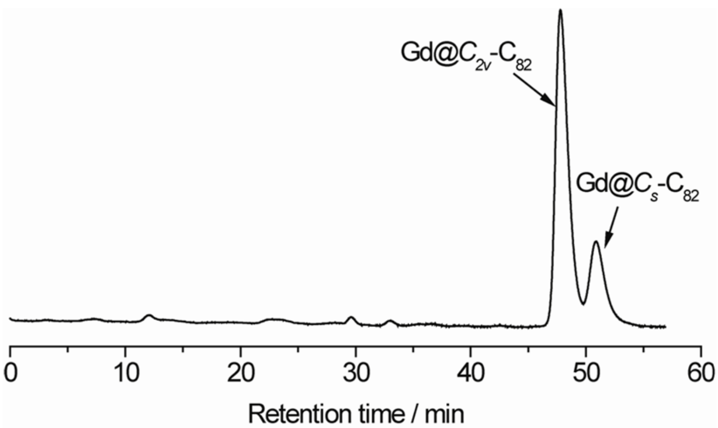

Figure S2. The second-step separation of Gd@C_{2v}-C_{82} on a Buckyprep column (Chromatographic column 20 × 250 mm; flow rate 12 mL/min; toluene as eluent).

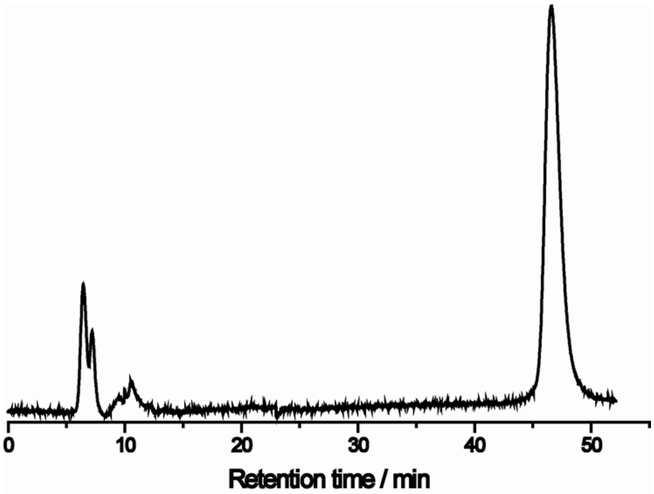

Figure S3. Chromatogram of the isolated Gd@C_{2v}-C_{82} on a Buckyprep column (Chromatographic column 20 × 250 mm; flow rate 12 mL/min; toluene as eluent).

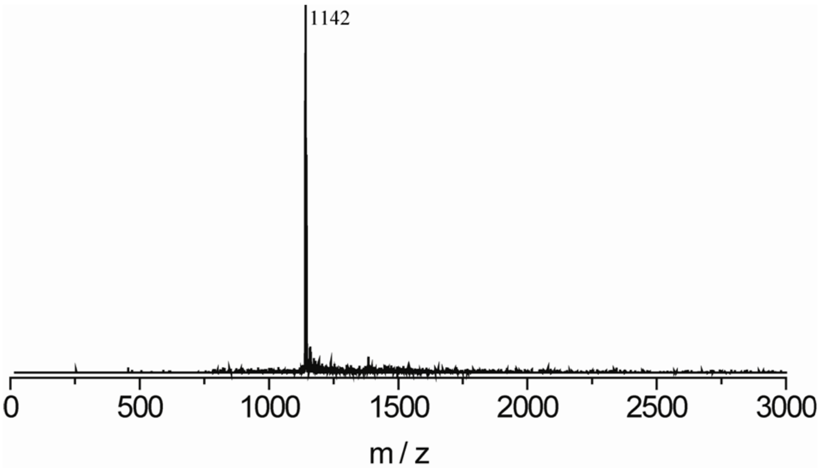

Figure S4. MALDI-TOF-MS spectrum of the isolated Gd@C_{2v}-C_{82}.

2. UV-Vis-NIR measurement

UV-Vis-NIR experiment was performed on a Shimadzu UV-2600 spectrometer. The purified Gd@C_{2v}-C_{82} sample was dissolved in ODCB with TBPA under different molar ratios.

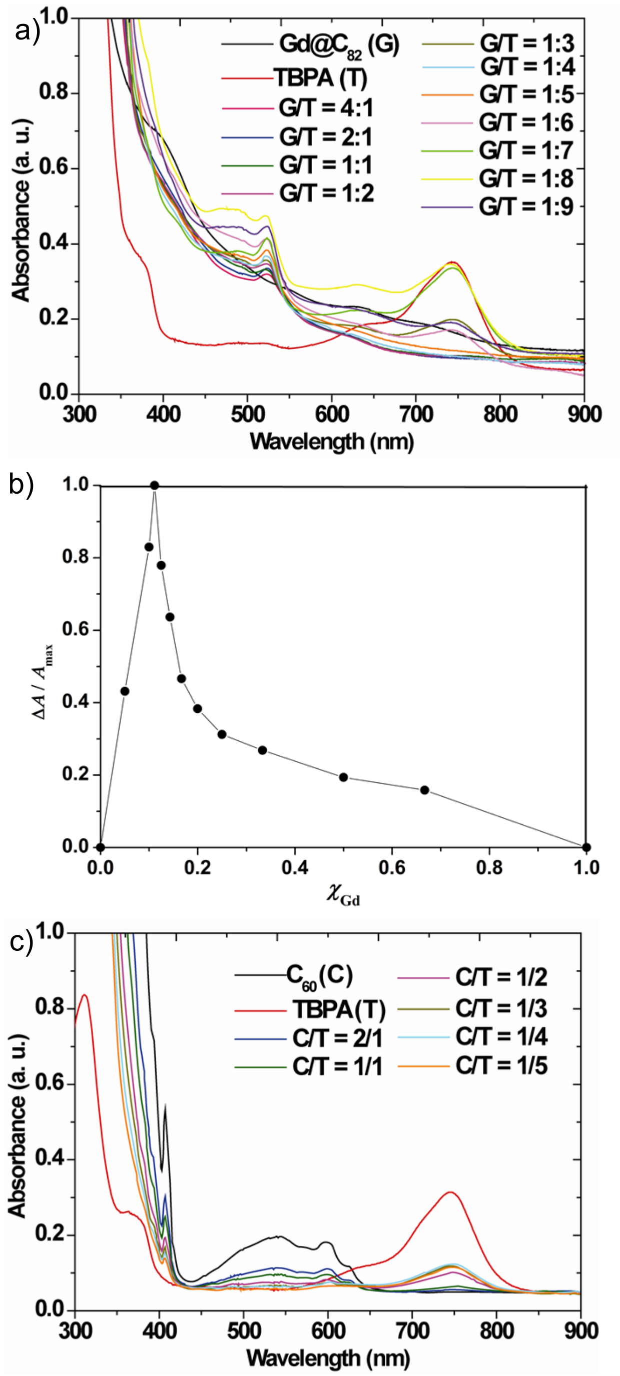

Figure S5. (a) The UV-Vis-NIR spectra of Gd@C_{82}, TBPA and their complex in ODCB solution. (b) Job's plot showing the relative absorption at 522 nm versus molar fractions of Gd@C_{82} (χ_{Gd}) in ODCB solution. (c) The UV-Vis-NIR spectra of C_{60}, TBPA and their complex in ODCB solution.

3. MALDI-TOF-MS

MALDI-TOF-MS measurement for Gd@C_{82}/TBPA complex was carried out on a Shimadzu Biotech Axima Assurance instrument, dithranol as matrix substance. From Figure S6, the single peak with mass-to-charge ratio of 1142 in positive and negative mode respectively indicated the complete structure of Gd@C_{82} ion in the ODCB solution by oxidation process.

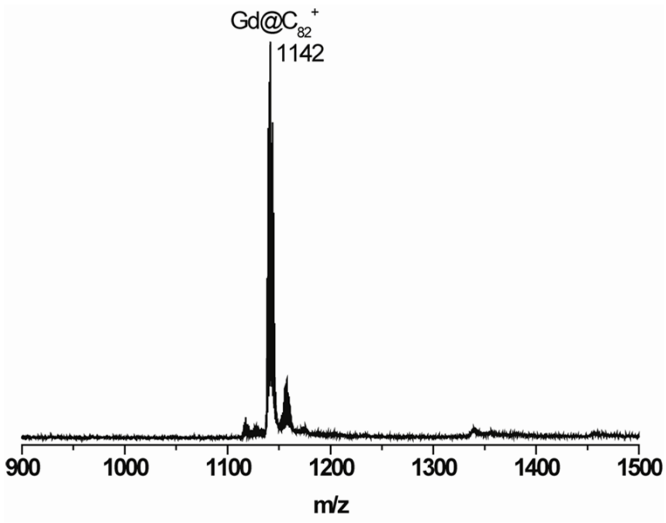

Figure S6. MALDI-TOF-MS profile of Gd@C_{82}/TBPA complex in positive mode, dithranol as matrix.

4. Electrochemical measurement.

Cyclic voltammetry was performed on a CHI660 electrochemical workstation. The experiment was carried out in ODCB solution with 0.05 M $(n\text{-Bu})_4NPF_6$ using three electrode system, glassy carbon as the working electrode, Pt wire and saturated calomel as the counter and reference electrodes, respectively. All the potentials were referred to the $E_{1/2}$ of Fc/Fc^+.

It can be seen from Table S1, Gd@C_{82} have three reduction potentials at -0.42, -1.43 and -2.38 V, respectively. It should be noted that the first reversible oxidation potential of Gd@C_{82} is at 0.10 V, and such low potential make it easy to form a gadofullerene salt complex through charge transfer process.

Table S1. Electrochemical potentials (V vs. Fc/Fc^+)[a] of Gd@C_{82} and TBPA.

	E_{ox1}	E_{red1}	E_{red2}	E_{red3}
Gd@C_{82}	0.10	-0.42	-1.43	-2.38[b]
TBPA	0.57	-0.61	-1.84[b]	

[a] the values of half-wave potentials for reversible redox processes.

[b] the peak potentials for irreversible processes.

5. Magnetization test

To 5 mL of ODCB solution with 4 mg of Gd@C_{82} (3.5 mM) was added about 25 mg of TBPA (30.6 mM). After a sonication treatment for 30 min, the mixture was filtered forming a dark blue solution. The product was precipitated by adding excessive amount of diethyl ether. The resulted powder was dried in vacuum at 50 °C for 12 h and sealed in a capsule with negligible magnetism.

Magnetization properties were performed on a Quantum Design MPMS XL-7 system at temperature from 5 K to 300 K in magnetic field of 0.1 Tesla for magnetic susceptibility measurement and 10 K with magnetic field up to 5 Tesla for M-H measurement. The investigated mass of the Gd@C_{82} and Gd@C_{82}/TBPA are 9.23 and 26.58 mg, respectively. Each sample was sealed in a capsule with negligible magnetism, the μ_{eff} were fitted to be 7.00 and 9.68 μ_B for Gd@C_{82} and Gd@C_{82}/TBPA, respectively (TBPA was diamagnetic as shown in Figure S7). Satisfactorily, the μ_{eff} of Gd@C_{82}/TBPA was enhanced by charge transfer between the fullerene cage and oxidizing agents compared with that of the parent Gd@C_{82} and even larger than the theoretical result (7.94 μ_B).[1-2] Figure S8 showed the M-T curves of these three compounds.

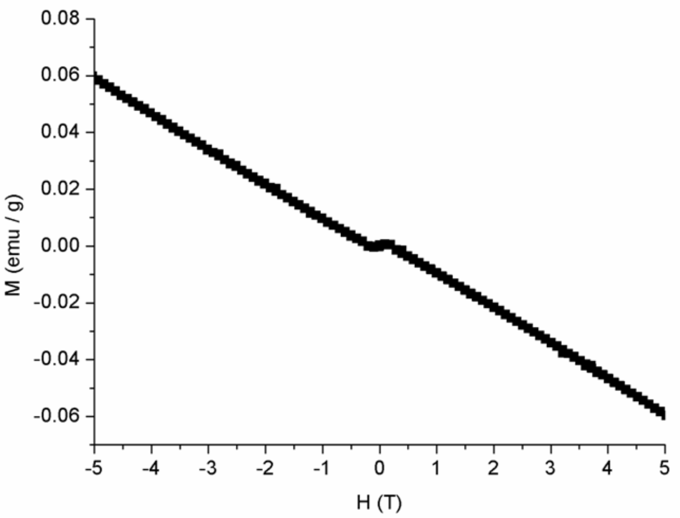

Figure S7. Magnetization (M) vs. field (H) plot of TBPA. The negative correlation of M vs. H showed a diamagnetic characteristic of TBPA.

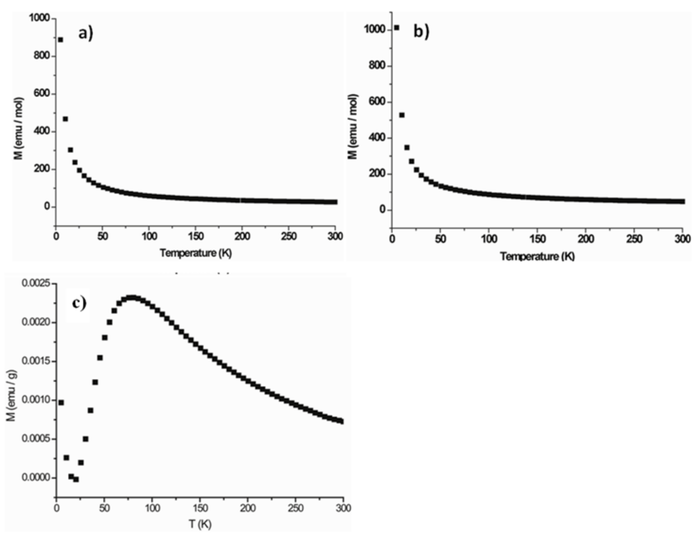

Figure S8. Magnetization (M) vs. temperature plots of (a) Gd@C_{82}, (b) Gd@C_{82}/TBPA, (c) TBPA.

6. ICP-AES test

ICP-AES experiment was performed on a SHIMADZU ICPE-90000 instrument to calibrate the investigated weight of Gd@C_{82} in Gd@C_{82}/TBPA complex as well as the composition of Gd@C_{82}/TBPA. The sample was dissolved in 2 mL of HNO_3, sonicated for 30 min and then transferred to a mixture of H_2SO_4/H_2O_2 (v/v = 4/1), sonicated for another 30 min. This acid solution was diluted 1000 times and then detected the Gd^{3+} and Sb^{5+}. The atomic ratio of Gd^{3+} to Sb^{5+} was about 1:8.

7. XPS measurement for Gd@C_{82}/TBPA complex

XPS of Gd@C_{82}/TBPA complex was performed on the Thermo Scientific ESCALab 250Xi using 200 W monochromated Al Kα radiation. The 500 μm X-ray spot was used for XPS analysis. The base pressure in the analysis chamber was about 3×10^{-10} mbar. Typically the hydrocarbon C1s line at 284.8 eV from adventitious carbon is used for energy referencing. Figure S9a and b show the Gd4d and Sb3d peak, respectively and c a schematic structure of the most stable complex of Gd@C_{82}/TBPA with a molar ratio of 1:8.

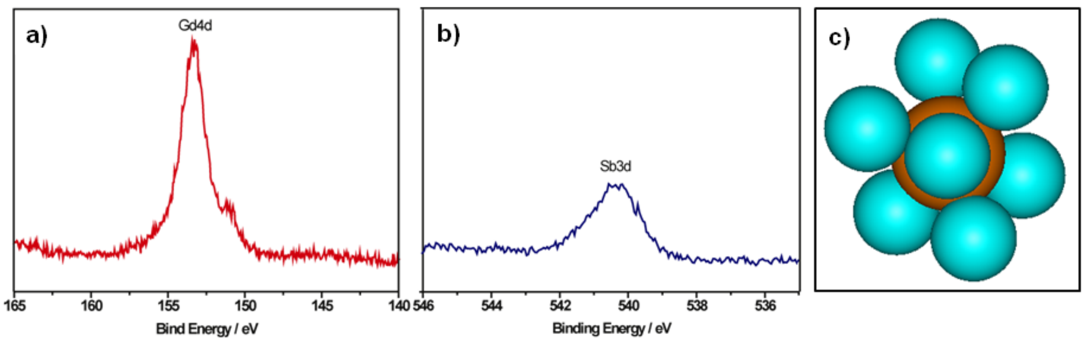

Figure S9. XPS spectra of (a) Gd4d peak and (b) Sb3d peak. (c) Schematic structure of Gd@C_{82}/TBPA complex. The orange ball in the centre represents Gd@C_{82} and the peripheral ball in blue refers TBPA.

8. XRD and TG-DTA measurements.

Figure S10 show the powder XRD patterns of Gd@C_{82}, TBPA and Gd@C_{82}/TBPA. It can be seen that the spectrum of Gd@C_{82} was featureless except for two envelope peaks and two weak peaks, while the XRD shape of Gd@C_{82}/TBPA was very similar with that of pristine TBPA.

TG-DTA measurement was performed to determine the stability of Gd@C_{82}/TBPA. As can be seen from Figure S11, the TGA curve of Gd@C_{82}/TBPA show only three stages which refer to the weight loss of solvent molecules (below 200 °C), TBPA and decomposition of carbon cage of Gd@C_{82}, whereas the TGA curve of TBPA exhibit six complex steps.

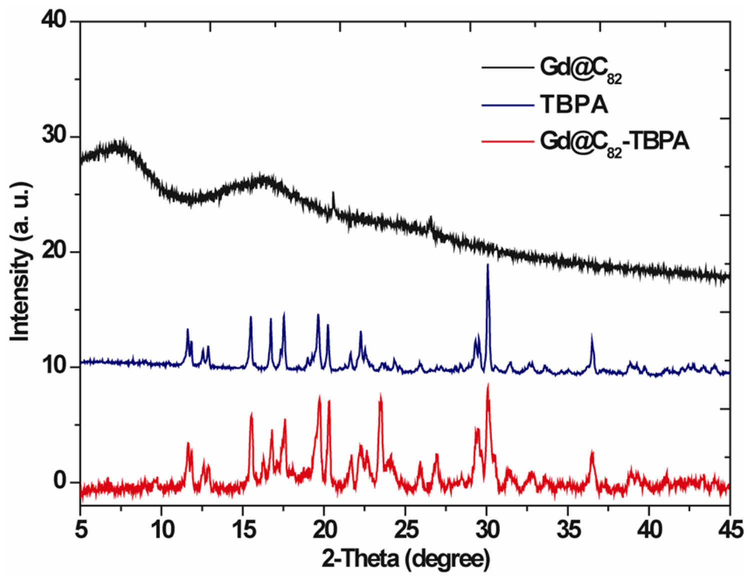

Figure S10. XRD spectra of (a) Gd@C_{82}, (b) TBPA and (c) Gd@C_{82}/TBPA complex.

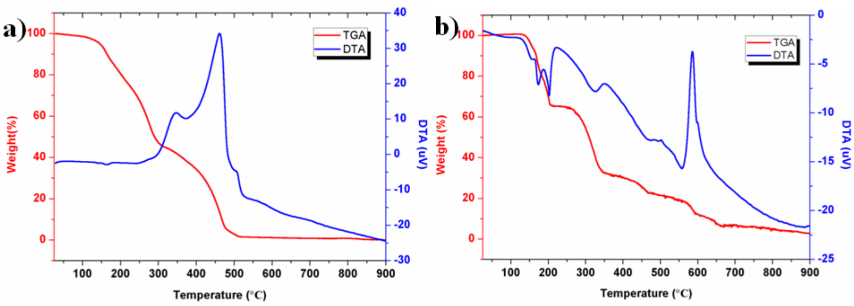

Figure S11. TG-DTA spectra of (a) Gd@C_{82}/TBPA and (b) TBPA.

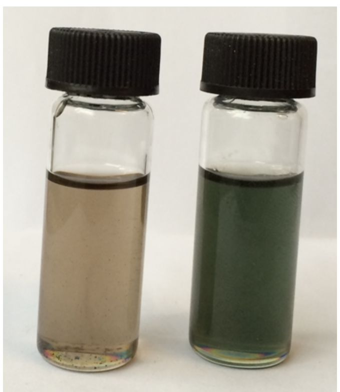

Figure S12. Aggregated Gd@C_{82} powder in ODCB (left) and ODCB solution of Gd@C82 with 1 eq. of TBPA (right).

9. Solubility test

The mass weight of Gd@C_{82}/TBPA powder for the solubility measurement experiment were as follow: 1.57, 1.06, 1.16, 1.69 and 1.16 mg, and then five kinds of solvent $CHCl_3$, MeCN, EtOAc, pyridine and THF were successively dropped until the powder was just dissolved completely. For comparison the solubility of Gd@C_{82} was also tested in these solvents as shown in Figure S13.

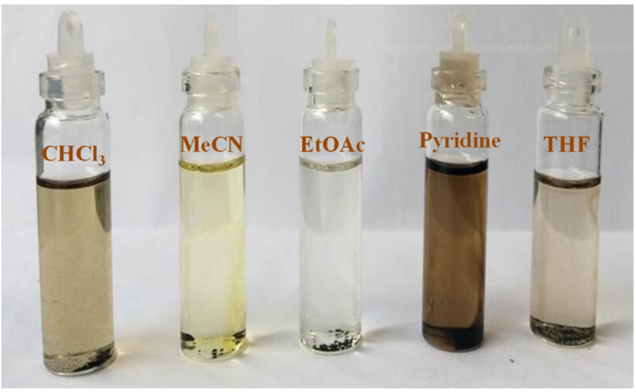

Figure S13. Optical images of solutions of Gd@C_{82} in $CHCl_3$, MeCN, EtOAc, Pyridine, and THF (from left to right in sequences).

10. Gd@C_{82}/TBPA hydrolysis experiment

About 1 mg of Gd@C_{82}/TBPA powder was suspended in 2mL of deionized water and sonicated for 30 min, then 2 mL of HCl was added and sonicated for another 30 min. Gd@C_{82} was extracted by ODCB and characterized by UV-vis spectroscopy. It can be seen from Figure S14 after hydrolysis the peak at 522 and 744 nm disappeared indicating the Gd@C_{82}/TBPA was decomposed and turned to pristine Gd@C_{82}.

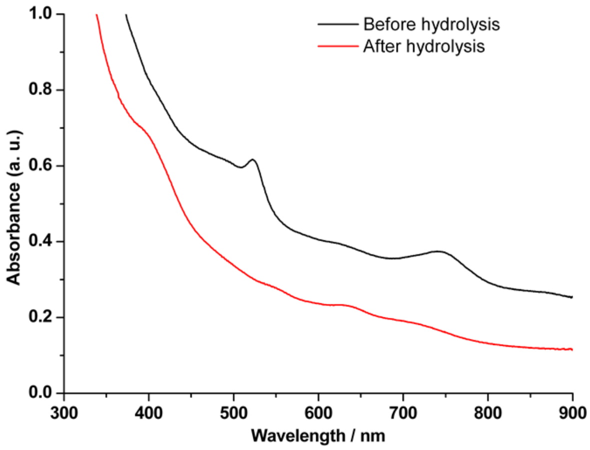

Figure S14. UV-vis spectra of Gd@C_{82}/TBPA before (black) and after (red) hydrolysis.

11. Electro-spinning fabrication and magnetic characterization of Gd@C_{82}/TBPA-PVP composite film

1.12 g of PVP ($M_n \approx$ 1 300 000) was dissolved in 10 mL of $CHCl_3$, by stirring for 10 h to form a uniform precursor blended solution, then 6.23 mg of Gd@C_{82}/TBPA powder was added and stirred for another 4 h. About 5 mL of the precursor solution was placed in a 10 mL syringe equipped with a blunt metal needle of 0.7 mm inner diameter. The solution feed rate was about 1.5 mL/h. A sheet of silver paper was used as the collector. The distance between the needle tip and collector was 15 cm, and the voltage was set at 20 kV.[3-6] Magnetic characterization of Gd@C_{82}/TBPA-PVP complex film was performed at the same conditions with Gd@C_{82}/TBPA complex. For comparison, PVP ($M_n \approx 30\ 000$) with weight ratio of 5 wt% and 7 wt% were prepared in the same manner, see Figure S15.

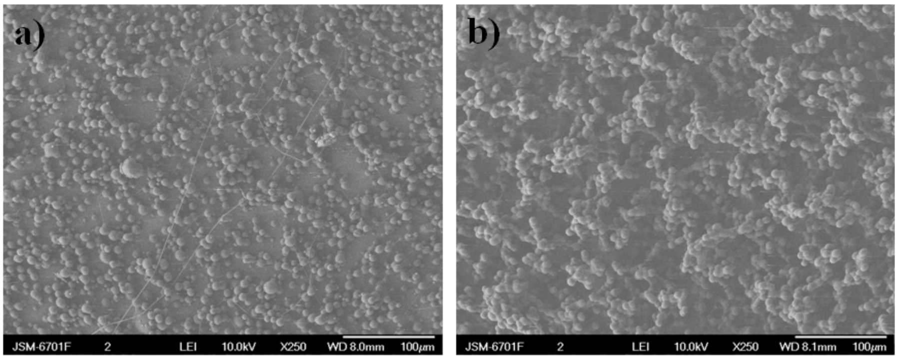

Figure S15. SEM images of the Gd@C_{82}/TBPA-PVP composite film fabricated by electrospinning with a PVP ($M_n \approx 30\ 000$) concentration of a) 5% and b) 7%.

12. EPR measurement

EPR experiment was performed on a Bruker E500 instrument. The spectra were recorded with X-band continuous wave at 173 K.

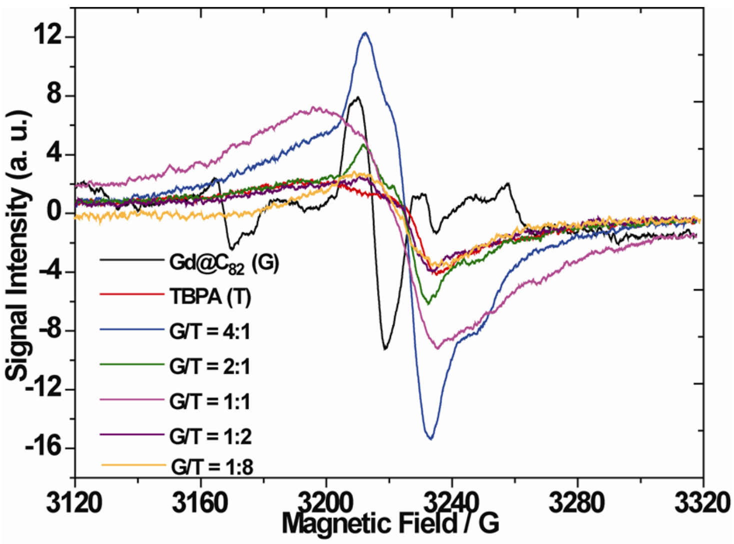

Figure S16. X-band EPR spectra of Gd@C_{82} and TBPA mixture measured at 173 K.

References:

1 H. Huang, S. Yang and X. Zhang, *J. Phys. Chem. B*, 1999, **103**, 5928-5932.

2 H. Funasaka, K. Sakurai, Y. Oda, K. Yamamoto and T. Takahashi, *Chem. Phys. Lett.*, 1995, **232**, 273-277.

3 H. Dong, N. Wang, L. Wang, H. Bai, J. Wu, Y. Zheng, Y. Zhao and L. Jiang, *ChemPhysChem*, 2012, **13**, 1153-1156.

4 J. Wu, N. Wang, Y. Zhao and L. Jiang, *J. Mater. Chem. A*, 2013, **1**, 7290-7305.

5 N. Wang, Y. Zhao and L. Jiang, *Macromol. Rapid. Comm.*, 2008, **29**, 485-489.

6 Q. Zhao, Z. Huang, C. Wang, Q. Zhao, H. Sun and D. Wang, *Mater. Lett.*, 2007, **61**, 2159-2163.